Supplement to "Energy and Mass-Number Dependence of Hadron-Nucleus Total Reaction Cross Sections" [J. Phys. Soc. Japan 85 (2016)]

Akihisa Kohama,[1] Kei Iida,[1,2] and Kazuhiro Oyamatsu[1,3]

[1]*RIKEN Nishina Center, RIKEN, 2-1 Hirosawa, Wako-shi, Saitama 351-0198, Japan*
[2]*Department of Natural Science, Faculty of Science, Kochi University, Kochi 780-8520, Japan*
[3]*Department of Human Informatics, Aichi Shukutoku University, 2-9 Katahira, Nagakute, Aichi, 480-1197, Japan*

We here summarize additional contents including several useful expressions. We use units in which $\hbar = c = 1$.

1. A Possible Relation to Density Distributions

In this section, we discuss where the black sphere (BS) radius, a, at $T_p \gtrsim 800$ MeV is located in the nuclear density distribution. We then compare the mass number dependence of $r_{\rm BS}$ with that of r_m.

1.1 Which Part is Probed?

Let us first define the critical nucleon density n_c as the density at $r = a$. We then deduce the values of a and n_c for ^{4}He, $^{\rm natu.}$C, ^{124}Sn, and $^{\rm natu.}$Pb from elastic scattering data at $T_p = 800$ MeV (see ref. 1 and references therein). The resultant values of n_c are listed in Table I. We find that in all the cases the BS radius is located in the surface region. We also find that n_c weakly depends on A in a manner that is consistent with $n_c \propto A^{-1/6}$. This dependence is discussed in Sec. 4 of ref. 2.

1.2 $r_{\rm BS}$ vs. r_m

In this subsection, we discuss the behavior of $r_{\rm BS} - r_m$ as a function of A at $T_p \gtrsim 800$ MeV. As we showed in ref. 3 (see Fig. 1), $r_{\rm BS} - r_m$ is consistent with zero for $A \gtrsim 50$, while $r_{\rm BS} - r_m$ is appreciably below zero for $A \lesssim 50$.

As we mentioned in ref. 3 and in Sec. 3.2 of ref. 2, the drastic change in the difference around $A \sim 50$ suggests a possible change in the form of the real nucleon density distribution; the rectangular distribution as assumed in deducing the rms radius $r_{\rm BS}$ may well simulate the real distribution at $A \gtrsim 50$, while for $A \lesssim 50$ the real distribution is quite different from the rectangular one in such a way that the portion of the real distribution farther than a is relatively large. This feature is suggested by the empirical charge distribution deduced from the electron-nucleus elastic scattering,[4] which shows a Gaussian-like form rather than a rectangular one for light nuclei.

This feature of the nucleon distribution is expected to be reflected by size-sensitive observables for which empirical data are available for stable nuclei ranging from light to heavy ones. Such observables include $1s$ states of pionic atoms and isoscalar giant resonance energies; the isoscalar part of the pion-nucleus optical potential[5] and the inertia associated with the resonances[6] are related to the nucleon distribution.

Table I. The values of n_c at $T_p = 800$ MeV.

Nucleus	n_c (fm^{-3})
$^{\rm natu.}$Pb	0.028
^{124}Sn	0.033
$^{\rm natu.}$C	0.044
^{4}He	0.060

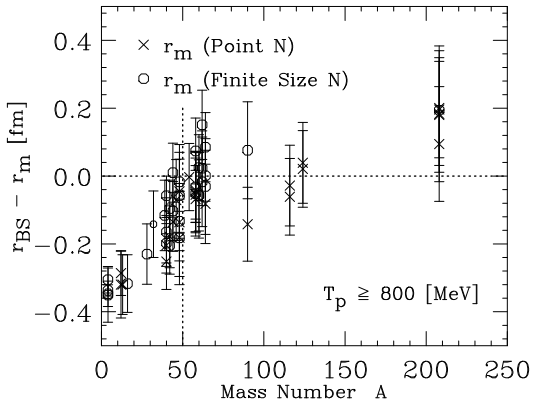

Fig. 1. The difference, $r_{\rm BS} - r_m$, as a function of mass number A (from Fig. 2 of ref. 3). The crosses (×) and the circles (○) are calculated from the corresponding values of r_m in Fig. 1 of ref. 3. The dotted line shows $r_{\rm BS} = r_m$ and $A = 50$.

To make the problem clearer, we adopt the two-parameter Fermi function as a typical nuclear density distribution. By expanding it in terms of $A^{1/3}$, we obtain the rms radius as (see Eq. (2-71) in p. 161 of ref. 7)

$$\langle r^2 \rangle^{1/2} = 0.93A^{1/3} + 1.78A^{-1/3} + \cdots \text{ fm}. \qquad (1.1)$$

From the above expression, we can understand that the first term of the right side corresponds basically to the BS scaling of $r_{\rm BS} = 0.94A^{1/3}$ fm, Eq. (3.3) of ref. 2. A part of the difference for $A \lesssim 50$ found in Fig. 1 comes from the second term of Eq. (1.1). A more systematic study in this direction was reported in ref. 8 (see also Sec. 4 in this supplement).

2. Connection with the Eikonal Approximation

In this section, we show the connection of our BS approximation of nuclei with the eikonal approximation, and summarize the key expressions for the purpose of completeness and clarification.

The scattering amplitude of proton-nucleus elastic scatter-

ing, $f(\mathbf{q})$, in the eikonal approximation is given by[9)]

$$f(\mathbf{q}) = ip \int_0^\infty bdb\ J_0(qb)\{1 - \exp[i\chi(b)]\}, \tag{2.1}$$

where $\mathbf{q}$ is the momentum transfer, $\mathbf{p}$ is the proton momentum in the c.m. frame, $\mathbf{b}$ is the impact parameter vector perpendicular to $\mathbf{p}$, $J_n(x)$ is the n-th order Bessel function, and

$$\chi(\mathbf{b}) = -\frac{1}{v}\int_{-\infty}^{\infty} dz'\ V_{\rm opt}(\mathbf{b} + \kappa z'), \tag{2.2}$$

is the phase-shift function with the velocity of an incident proton $v\left(= |\mathbf{p}|/\sqrt{\mathbf{p}^2 + m_p^2}\right)$, the proton-nucleus optical potential $V_{\rm opt}(\mathbf{r})$, and $\kappa = \mathbf{p}/|\mathbf{p}|$. We then obtain the differential cross section of elastic scattering as

$$\frac{d\sigma_{\rm elastic}}{d\Omega} = |f(\mathbf{q})|^2. \tag{2.3}$$

Within the $t\rho$ approximation to the optical potential,[9)] the phase-shift function reads

$$\chi(b) = \frac{2\pi}{p}\sum_{N=n,p} f_{pN}(\mathbf{0})\int_{-\infty}^{\infty} dz'\ \rho_N(\mathbf{b} + \kappa z'), \tag{2.4}$$

where $f_{pN}(\mathbf{0})$ is the proton-nucleon scattering amplitude in the forward direction, and $\rho_N(\mathbf{r})$ is the N nucleon one-body density distribution. Expression (2.4) corresponds to the optical-limit approximation in the Glauber approximation. The imaginary part of $f_{pN}(\mathbf{0})$ is related to $\sigma_{pN}^{\rm total}$ by the optical theorem as

$$\mathrm{Im} f_{\rm pN}(\mathbf{0}) = \frac{p}{4\pi}\sigma_{pN}^{\rm total}. \tag{2.5}$$

Using the scattering amplitude of Eq. (2.1) in the forward direction, we obtain the total cross section via the optical theorem for proton-nucleus scattering as

$$\begin{aligned}\sigma_{\rm total} &= \frac{4\pi}{p}\mathrm{Im} f(\mathbf{0}) \\ &= 4\pi\int_0^\infty bdb\ \{1 - \mathrm{Re}\ \exp[i\chi(b)]\}.\end{aligned} \tag{2.6}$$

Note that this allows for the contribution from the strong interaction alone. The total elastic scattering cross section can be obtained from Eq. (2.3) as

$$\sigma_{\rm elastic} = 2\pi\int_0^\infty bdb\ |\exp[i\chi(b)] - 1|^2, \tag{2.7}$$

which in turn leads to the absorption cross section,

$$\begin{aligned}\sigma_{\rm abs} &= \sigma_{\rm total} - \sigma_{\rm elastic} \\ &= 2\pi\int_0^\infty bdb\ \{1 - |\exp[i\chi(b)]|^2\} \\ &= 2\pi\int_0^\infty bdb\ \{1 - \exp[-2\mathrm{Im}\chi(b)]\}.\end{aligned} \tag{2.8}$$

In the strongly absorptive limit of the eikonal approximation with the density distribution whose cutoff is equal to the BS radius a, we can write the phase-shift function, $\chi(b)$, as

$$\exp[i\chi(b)] = \theta(b - a). \tag{2.9}$$

Then, the scattering amplitude becomes the Fraunhofer scattering amplitude in optics:

$$f(\mathbf{q}) = ipaJ_1(qa)/q. \tag{2.10}$$

Using expression (2.9), we obtain from Eq. (2.6)

$$\sigma_{\rm total} = 2\pi a^2. \tag{2.11}$$

Also, we obtain

$$\sigma_{\rm elastic} = \pi a^2 \tag{2.12}$$

and

$$\sigma_{\rm abs} = \pi a^2. \tag{2.13}$$

In this framework, the absorption cross section $\sigma_{\rm abs}$ corresponds to the BS cross section $\sigma_{\rm BS} = \pi a^2$ and thus can be identified with the total reaction cross section σ_R of proton-nucleus scattering. This is the formal relation of the BS approximation with the eikonal approximation.

As described in Sec. 2.2 of ref. 2, we determine a by fitting the angle of the first elastic diffraction peak calculated for proton diffraction by a circular black disk of radius a to the measured value, which is the essential difference from the classical BS approximation.

3. Derivation of the BS Cross-Section Formula

In this section, we describe how to derive the BS cross-section formula. This formula was originally reported in ref. 10. The present description is partly a repetition of that work, but aims at being more detailed.

We express the energy dependence of $\sigma_{\rm BS}$ ($\equiv \pi a^2$), Eq. (2.8) of ref. 2, as

$$\begin{aligned}\tilde{\sigma}_{\rm BS}(T_p) &= \pi a(T_p)^2 \\ &= \pi a_0^2\left(1 + \frac{\Delta a}{a_0}\right)^2,\end{aligned} \tag{3.1}$$

where $\Delta a \equiv a(T_p) - a_0$ is responsible for the energy dependence of $\tilde{\sigma}_{\rm BS}$. a_0 is the value of a determined at 800 MeV in the same way as in Sec. 2.2 of ref. 2. In this setting, we assume that the incident protons are point particles, leading to vanishing contribution from the proton size to a. This is reasonable since the measured proton-proton reaction cross section is relatively small at T_p less than $\sim$ 1000 MeV.

In deriving the expression for Δa, we introduce the "optical" depth or thickness of a target nucleus. As originally introduced in astrophysics,[11)] the optical depth, or optical thickness, is a measure of transparency and is defined as the negative logarithm of the fraction of radiation that is not scattered or absorbed on a path. In the present "optical" depth, we consider the fraction of projectiles that are transparent through the target nucleus, because the BS radius a corresponds to a critical radius inside which the protons are attenuated in a target nucleus.

In the context of the conventional nuclear scattering theory, as one can see from expression (2.8), the fraction is in proportion to the flux attenuation factor, which can be obtained from $\mathrm{Im}\,\chi(b)$, Eq. (2.4), as

$$\begin{aligned}|\exp[\chi(b)]|^2 &= \exp[-2\mathrm{Im}\chi(b)] \\ &= \exp\left[-\sum_{N=n,p}\sigma_{pN}^{\rm total}\int_{-\infty}^{\infty} dz'\ \rho_N(\mathbf{b} + \kappa z')\right].\end{aligned} \tag{3.2}$$

Thus, the nuclear optical depth for absorption of proton pro-

jectiles in the conventional scattering theory can be symbolically expressed as

$$\tau_{\rm conv} = \int_l dl \left[\sigma_{pn}^{\rm total}\rho_n(\mathbf{r}) + \sigma_{pp}^{\rm total}\rho_p(\mathbf{r})\right], \tag{3.3}$$

where l is the proton trajectory.

The empirical relation that $\sigma_R \simeq \sigma_{\rm BS}$ suggests that expression (3.3) amounts to a critical value when the nearest distance between the proton trajectory and the nuclear center is a. Let us now approximate the trajectory by a straight line (Fig. 5 of ref. 2) although it is slightly distorted by the Coulomb repulsion.

In the present framework, instead of Eq. (3.3), we introduce the *effective* nuclear optical depth τ, Eq. (4.2) of ref. 2. By approximating the nuclear density distribution as a trapezoidal form as shown in Fig. 5 of ref. 2, we express L' by

$$L' = 2\sqrt{R^2 - a^2}. \tag{3.4}$$

In the trapezoidal form of the nucleon distributions, we set the length of the bottom, R, the surface thickness, D, and the length of the top, $R-D$, in such a way as to reproduce a typical behavior of the distributions deduced from elastic scattering data off stable nuclei. The surface thickness D is the thickness outside of the plateau of the density distribution of density ρ_0.

Let us now consider the deviation of ΔX of X ($= \bar\sigma_{pN}^{\rm total}, a, n_c,$ and L') from the value X_0 at $T_p = 800$ MeV under the condition that the nuclear optical depth τ is independent of T_p. As long as $T_p > 100$ MeV, $\Delta\bar\sigma_{pN}[= \bar\sigma_{pN}^{\rm total}(T_p) - \bar\sigma_{pN0}^{\rm total}]$ is sufficiently small to validate the following expression up to first order in the deviations

$$\tau\frac{\Delta\bar\sigma_{pN}^{\rm total}}{(\bar\sigma_{pN0}^{\rm total})^2} \approx -n_{c0}\Delta L' - L_0'\Delta n_c, \tag{3.5}$$

which follows from

$$\Delta\left(\frac{\tau}{\bar\sigma_{pN}^{\rm total}}\right) = \Delta(n_c L'). \tag{3.6}$$

$\Delta L'$ in Eq. (3.5) can be rewritten as

$$\Delta L' \approx \left.\frac{dL'}{da}\right|_0 \Delta a. \tag{3.7}$$

Because of the assumed trapezoidal distribution, one can obtain

$$\Delta n_c = -\frac{\rho_0}{D}\Delta a. \tag{3.8}$$

For the estimation of D, we consider the slope to be linear near the half-density radius as the simplest approximation. For example, as the nuclear density distribution $\sum_{N=n,p}\rho_N(\mathbf{r})$, we adopt the two-parameter Fermi distribution,

$$\rho_{\rm 2pF}(r) = \frac{\rho_{f0}}{1+\exp{(r-c)/z}}, \tag{3.9}$$

where c is the half-density radius, and z determines the diffuseness. Typically, they are parameterized as $c \simeq 1.3A^{1/3}$ fm and $z \simeq 0.5$ fm, respectively. The condition that the slope should be the same at $r = c$ reads

$$\left.\frac{d\rho_{\rm 2pF}(r)}{dr}\right|_{r=c} = -\rho_{f0}\frac{1}{4z} = \frac{\rho_0}{D}. \tag{3.10}$$

Assuming $\rho_{f0} \simeq \rho_0$, we obtain $D = 4z$. The value of $z = 0.55$ fm corresponds to $D = 2.2$ fm, which is taken throughout the present work.

Combining Eqs. (3.5), (3.7), and (3.8), one can derive the relation between $\Delta\bar\sigma_{pN}$ and Δa as

$$\begin{aligned}\frac{\Delta a}{a_0} &= \left(\frac{\rho_0}{D}L_0' - \left.\frac{dL'}{da}\right|_0 n_{c0}\right)^{-1}\frac{\tau}{a_0}\frac{\Delta\bar\sigma_{pN}^{\rm total}}{(\bar\sigma_{pN0}^{\rm total})^2} \\ &= \left(\frac{\rho_0 a_0}{Dn_{c0}} - \frac{a_0}{L_0'}\left.\frac{dL'}{da}\right|_0\right)^{-1}\frac{\Delta\bar\sigma_{pN}^{\rm total}}{\bar\sigma_{pN0}^{\rm total}}.\end{aligned} \tag{3.11}$$

We thus obtain the BS cross-section formula as

$$\tilde\sigma_{\rm BS}(T_p) = \pi a_0^2\left[1 + \left(\frac{\rho_0 a_0}{Dn_{c0}} - \frac{a_0}{L_0'}\left.\frac{dL'}{da}\right|_0\right)^{-1}\frac{\Delta\bar\sigma_{pN}^{\rm total}}{\bar\sigma_{pN0}^{\rm total}}\right]^2, \tag{3.12}$$

where $L_0' = 2\sqrt{R^2 - a_0^2}$, $\rho_0 = 0.16$ fm^{-3}, and n_{c0} is given by

$$n_{c0} = \tau/(L_0'\bar\sigma_{pN0}^{\rm total}). \tag{3.13}$$

Here we choose $\tau = 0.9$ in such a way as to reproduce the values of n_{c0} that are summarized in Table I in Sec. 1. For $\sigma_{pp}^{\rm total}$ and $\sigma_{pn}^{\rm total}$, see Appendix A of ref. 2.

We now proceed to express dL'/da at $T_p = 800$ MeV and the length R. In doing so, we first note the normalization condition for the assumed trapezoidal distribution,

$$A = \frac{4\pi\rho_0}{3}\left(R^3 - \frac{3}{2}DR^2 + D^2R - \frac{1}{4}D^3\right). \tag{3.14}$$

While we could solve this in R analytically, we solve it approximately for later convenience. One can seek an approximate solution to Eq. (3.14) by setting

$$R = R_0 + D/2 + \delta R, \tag{3.15}$$

with

$$R_0 = [3A/(4\pi\rho_0)]^{1/3}, \tag{3.16}$$

and assuming that δR is small. One thus obtains

$$R \simeq R_0 + \frac{D}{2} - R_0\left(1 + \frac{12R_0^2}{D^2}\right)^{-1}. \tag{3.17}$$

From this expression, δR can be shown to be small even for light elements. Hereafter we substitute expression (3.17) into the cross-section formula (3.12) through L'.

We can then obtain dL'/da from Eqs. (3.4) and (3.17). The expression for dL'/da is given by

$$\begin{aligned}\frac{dL'}{da} &= \frac{2}{L'}\frac{d}{da}(R^2 - a^2) \\ &= \frac{4}{L'}(R\frac{dR}{da} - a).\end{aligned} \tag{3.18}$$

Since $dR/da = 0$, we can estimate the values of dL'/da at $T_p = 800$ MeV in Eq. (3.12) from

$$\left.\frac{dL'}{da}\right|_0 = -\frac{4}{L_0'}a_0. \tag{3.19}$$

Note that in our previous paper,[10] we have mistakenly assumed $dR_0/da|_0 = R_0/a_0$ in calculating $dL'/da|_0$. The relevant corrections, which are included in Eq. (3.19), act to decrease the magnitude of Δa, but change the value of $\tilde\sigma_{\rm BS}(T_p)$ by an amount of the order of typical experimental error bars

at most.

4. Comparison between Various Radii of Stable Nuclei

In this section, we briefly review ref. 8, which explains the physics underlying the fact that the A dependence of the difference between the rms BS radius $r_{\rm BS}$ and matter radius r_m of stable nuclei changes abruptly around $A = 50$ as shown in Fig. 1. In ref. 8, the author concluded that this abrupt change stems from the combined effects of the surface diffuseness and neutron skin.

Let us now recall that the BS radius a behaves almost completely as $A^{1/3}$ [3] [see Eq. (3.3) of ref. 2]. We thus find that the abrupt change of the A dependence of $r_{\rm BS} - r_m$ is controlled by r_m. To see the A dependence of r_m, we consider the rms charge radius r_c as a reference. This is because r_c is empirically well-known,[4] leading to various formulas as function of A.[12] For example, one can approximate the charge density distribution by the two-parameter Fermi distribution, leading to expansion with respect to A like Eq. (1.1). Instead, we here use the trapezoidal charge density distribution, which allows us to analytically obtain the rms charge radii. In fact, by assuming that the proton point density distribution is proportional to the trapezoidal matter density distribution given in Sec. 3 in this supplement, we obtain

$$r_c^t = \left[\frac{3}{5R_0^3}\left(3R^3 - \frac{15}{2}DR^4 + 10D^2R^3 - \frac{15}{2}D^3R^2 + 3D^4R - \frac{1}{2}D^5\right) + \frac{3}{2}r_p^2\right]^{1/2}, \tag{4.1}$$

where R_0 and R are given by Eqs. (3.16) and (3.17), respectively, and $r_p = 0.65$ fm allows for the proton charge radius.[13] Note that this expression well reproduces the overall empirical data for r_c.

We proceed to compare $r_{\rm BS}$, $\tilde{r}_m$, and r_c for stable nuclei. In Fig. 2 we plot $\tilde{r}_m - r_{\rm BS}$, where $\tilde{r}_m$ is deduced from the experimental overall differential cross sections for proton elastic scattering via optical potential models, and $r_{\rm BS}$ is obtained from the measured peak angles in the same differential cross sections. The data are the same as in Fig. 1, but here for the data for r_m that have the nucleon size ignored, we reevaluate it as $\tilde{r}_m^2$ by adding $(3/2)r_p^2$ to the original r_m^2 for the sake of consistency with the definition of r_c. For comparison, we also plot $r_c - r_{\rm BS}$, where r_c is taken from ref. 4, together with $r_c^t - 0.94A^{1/3}$ fm. As can be seen from the figure, $r_c^t - 0.94A^{1/3}$ fm well simulates the empirical behavior of $r_c - r_{\rm BS}$. For $A \lesssim 50$, $\tilde{r}_m - r_{\rm BS}$ is positive and decreases with A, a feature that comes from the contribution of the surface diffuseness to $\tilde{r}_m$. We remark that in this region, r_c is almost indistinguishable from $\tilde{r}_m$, and that the nuclear surface occupies a large portion of the density distribution for light nuclei. For $A \gtrsim 50$, on the other hand, $\tilde{r}_m - r_{\rm BS}$ is consistent with zero, while $\tilde{r}_m$ is systematically larger than r_c. The latter feature almost certainly originates from the neutron skin thickness r_{np}, i.e., the difference in the rms radius between the neutron and proton density distributions, which develops as the beta stability line deviates from $Z = A/2$ into a neutron-rich regime. In fact, $\tilde{r}_m - r_c \approx (1 - Z/A)r_{np}$.

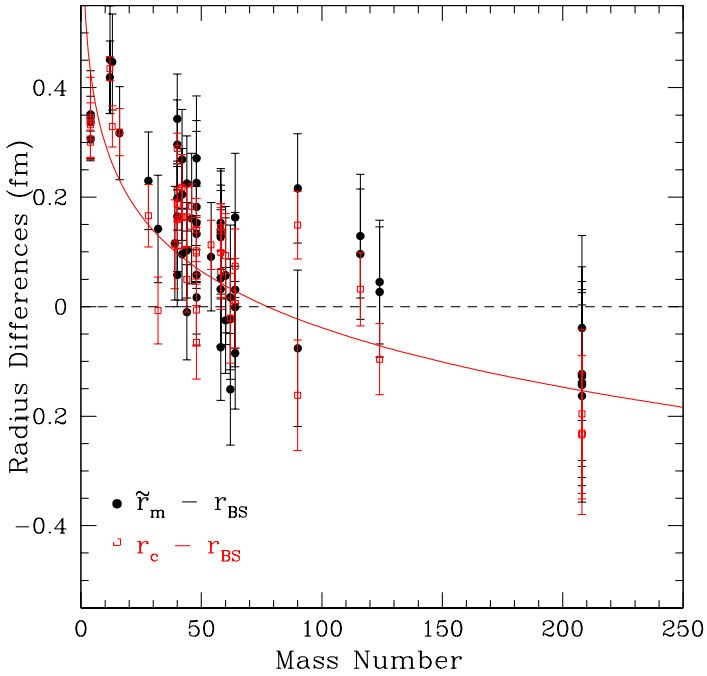

Fig. 2. (Color online) Empirical radius differences, $\tilde{r}_m - r_{\rm BS}$ (circles) and $r_c - r_{\rm BS}$ (squares), obtained for stable nuclei. The data for $\tilde{r}_m$ and $r_{\rm BS}$ adopted here are the same as in Fig. 1, but here the nucleon size is included for any $\tilde{r}_m$. For comparison, we plot $r_c^t - 0.94A^{1/3}$ fm in solid curve.

5. Supplementary Information for Appendix B: Scattering with a Square-Well Potential of Finite Strength

We here give additional expressions for scattering amplitudes and absorption cross sections that arise from the potential (B.1) of ref. 2.

5.1 *Scattering Amplitude*

Let us consider the derivation of the analytic expression for the scattering amplitude. From Eq. (2.1), we obtain

$$\begin{aligned} f(\mathbf{q}) &= ip\int_0^{\bar{a}} bdb\, J_0(qb) \times\left\{1 - \exp\left[-\frac{2(W_0 + iV_0)}{v}\sqrt{\bar{a}^2 - b^2}\right]\right\} \\ &= ip\int_0^{\bar{a}} xdx\, J_0\left(q\sqrt{\bar{a}^2 - x^2}\right) \times\{1 - \exp[-2(c_2 + ic_1)x]\} \\ &= ip(I_0 - I_c + iI_s), \end{aligned} \tag{5.2}$$

with $x = \sqrt{\bar{a}^2 - b^2}$, $c_1 = V_0/v$, $c_2 = W_0/v$,

$$I_0 = \int_0^{\bar{a}} xdx\, J_0\left(q\sqrt{\bar{a}^2 - x^2}\right) \tag{5.3}$$

$$\begin{aligned} I_c &= \int_0^{\bar{a}} xdx\, J_0\left(q\sqrt{\bar{a}^2 - x^2}\right) e^{-2c_2x}\cos(2c_1x) \\ &= -\frac{1}{2}\,{\rm Re}\frac{\partial}{\partial c_2} I_g, \end{aligned} \tag{5.4}$$

$$I_s = \int_0^{\bar{a}} xdx\, J_0\left(q\sqrt{\bar{a}^2 - x^2}\right) e^{-2c_2x}\sin(2c_1x)$$

$$= -\frac{1}{2}\,\mathrm{Im}\frac{\partial}{\partial c_2} I_g, \tag{5.5}$$

where

$$I_g = \int_0^{\bar{a}} dx\, J_0\left(q\sqrt{\bar{a}^2 - x^2}\right) \exp[-2(c_2 + ic_1)x]. \tag{5.6}$$

5.2 *Effect of Neutron Skin*

For future research involved, it could be significant to approach unstable neutron-rich nuclei. We thus extend the eikonal approximation based on the potential (B.1) of ref. 2 to the case of $a_n > a_p$, where a_n and a_p are the potential cut-off scales for neutrons and protons, respectively, as done in ref. 14. For simplicity, we confine ourselves to the case of $(a_n - a_p)/a_n \ll 1$. In this case, as we shall see, the reaction cross section (B.2) of ref. 2 includes a term that depends exponentially on the effective neutron skin thickness $a_n - a_p$.

Let us set the radius and density of the proton (neutron) distribution for a nucleus of given A and Z to be the same as a_p (a_n) and uniform at $\rho_{p0} = 3Z/(4\pi a_p^3)$ ($\rho_{n0} = 3(A-Z)/(4\pi a_n^3)$). Within the $t\rho$ approximation to the optical potential, the phase-shift function $\chi(b)$ given by Eq. (2.2) can be decomposed into

$$\chi(b) = \chi_{pp}(b) + \chi_{pn}(b), \tag{5.7}$$

where the imaginary part can be expressed as

$$\begin{aligned}\mathrm{Im}[\chi_{pp}(b) + \chi_{pn}(b)] &= \sigma_{pp}^{\mathrm{total}}\rho_{p0}\sqrt{a_p^2 - b^2}\,\theta(a_p - b) \\ &+ \sigma_{pn}^{\mathrm{total}}\rho_{n0}\sqrt{a_n^2 - b^2}\,\theta(a_n - b).\end{aligned} \tag{5.8}$$

By substitute Eq. (5.8) into Eq. (2.8), we obtain

$$\begin{aligned}\sigma_{\mathrm{abs}} &= \pi a_n^2 \\ &\quad -2\pi\int_0^{a_p} bdb\exp[-\zeta_p\sqrt{a_p^2 - b^2} \\ &\qquad -\zeta_n\sqrt{a_n^2 - b^2}] \\ &\quad -2\pi\int_{a_p}^{a_n} bdb\exp[-\zeta_n\sqrt{a_n^2 - b^2}]\end{aligned} \tag{5.9}$$

where $\zeta_p = 2\sigma_{pp}^{\mathrm{total}}\rho_{p0}$ and $\zeta_n = 2\sigma_{pn}^{\mathrm{total}}\rho_{n0}$. For later convenience, we define

$$\bar{\zeta} = \zeta_p + \zeta_n \tag{5.10}$$

In Eq. (5.9), we refer to minus the second term as (I) and to minus the third term as (II).

Since it is hard to analytically calculate (I), we will estimate the upper and lower limits of (I). Putting $y = a_p^2$ and $y_0 = a_n^2$, as well as keeping a_p and a_n being close in mind, via the mean-value theorem, we can write

$$\begin{aligned}f(y) &= \sqrt{y - b^2} \\ &= f(y_0) + f'(y_0 + c(y - y_0))(y - y_0),\end{aligned} \tag{5.11}$$

where $f' = df/dy$, and c is a number that satisfies $0 < c < 1$, while depending on b. The second term of Eq. (5.11) satisfies the following inequalities:

$$\begin{aligned}f'(y_0 + c(y - y_0)) &= \frac{1}{2\sqrt{y_0 + c(y - y_0) - b^2}} \\ &= \frac{1}{2\sqrt{(1-c)y_0 + cy - b^2}} \\ &< \frac{1}{2\sqrt{(1-c)(y_0 - y)}} \\ &< \frac{1}{\sqrt{y_0 - y}}.\end{aligned} \tag{5.12}$$

For the first inequality, we use the relation, $cy - b^2 \geq cy - y$ for $0 \leq b \leq a_p$. For the last inequality, we refer to the range of c as a function of b as shown in Table II. Then, Eq. (5.11) becomes

$$\sqrt{a_p^2 - b^2} > \sqrt{a_n^2 - b^2} - \sqrt{a_n^2 - a_p^2}, \tag{5.13}$$

and we can obtain in the case of strong absorption

$$\begin{aligned}\mathrm{(I)} &\ll 2\pi\int_0^{a_p} bdb\exp\left(-\bar{\zeta}\sqrt{a_n^2 - b^2} + \zeta_p\sqrt{a_n^2 - a_p^2}\right) \\ &= \exp\left(\zeta_p\sqrt{a_n^2 - a_p^2}\right) \\ &\quad \times 2\pi\int_0^{a_p} bdb\exp\left(-\bar{\zeta}\sqrt{a_n^2 - b^2}\right),\end{aligned} \tag{5.14}$$

where $\ll$ means that the left side is exponentially smaller than the right side.

Changing the variable of integration via $x = \sqrt{a_n^2 - b^2}$ ($xdx = -bdb$), we rewrite Eq. (5.14) as

$$\begin{aligned}\mathrm{(I)} &\ll \exp\left(\zeta_p\sqrt{a_n^2 - a_p^2}\right) \\ &\quad \times 2\pi\int_{\sqrt{a_n^2 - a_p^2}}^{a_n} xdx\exp(-\bar{\zeta}x).\end{aligned} \tag{5.15}$$

Then we can analytically calculate the integration in Eq. (5.15) using

$$\begin{aligned}\int_0^a xdx\ \exp(-bx) &= (1/b^2)[1 - (ab+1)\exp(-ab)], \\ &\quad (a, b > 0).\end{aligned} \tag{5.16}$$

The result is

$$\begin{aligned}&2\pi\int_{\sqrt{a_n^2 - a_p^2}}^{a_n} xdx\exp(-\bar{\zeta}x) \\ &= \frac{2\pi}{\bar{\zeta}^2}\left[1 - (a_n\bar{\zeta} + 1)\exp(-a_n\bar{\zeta})\right] \\ &\quad -\frac{2\pi}{\bar{\zeta}^2}\left[1 - \left(\bar{\zeta}\sqrt{a_n^2 - a_p^2} + 1\right)\exp\left(-\bar{\zeta}\sqrt{a_n^2 - a_p^2}\right)\right]. \\ &= \frac{2\pi}{\bar{\zeta}^2}\left(\bar{\zeta}\sqrt{a_n^2 - a_p^2} + 1\right)\exp\left(-\bar{\zeta}\sqrt{a_n^2 - a_p^2}\right)\end{aligned}$$

Table II. The behavior of c as a function of b.

b	0		a_p
$c(b)$	$(3a_n + a_p)/[4(a_n + a_p)]$	↗	3/4

$$-\frac{2\pi}{\bar{\zeta}^2}(a_n\bar{\zeta}+1)\exp\left(-a_n\bar{\zeta}\right). \tag{5.17}$$

In the same way as above, on the other hand, we can rewrite (II) as

$$\begin{aligned}(\mathrm{II}) &= 2\pi\int_{a_p}^{a_n} bdb\exp\left(-\zeta_n\sqrt{a_n^2-b^2}\right)\\ &= 2\pi\int_0^{\sqrt{a_n^2-a_p^2}} xdx\exp(-\zeta_n x)\\ &= \frac{2\pi}{\zeta_n^2}\left[1-(\zeta_n\sqrt{a_n^2-a_p^2}+1)\exp\left(-\zeta_n\sqrt{a_n^2-a_p^2}\right)\right].\end{aligned} \tag{5.18}$$

When one retains corrections to the BS limit ($\sigma_{pN}^{\mathrm{tot}}\to\infty$) by transparency of the skin region, (I) is negligible compared with (II). Thus, the absorption cross section (5.9) has a form

$$\begin{aligned}\sigma_{\mathrm{abs}} &\simeq \pi a_n^2\\ &\quad -\frac{2\pi}{\zeta_n^2}\left[1-\left(1+\zeta_n\sqrt{a_n^2-a_p^2}\right)e^{-\zeta_n\sqrt{a_n^2-a_p^2}}\right]\\ &\leq \pi a_n^2.\end{aligned} \tag{5.19}$$

It is instructive to note that Eq. (5.19) reduces to πa_n^2 in the BS limit. For large but finite values of ζ_n, the remaining term in the right side of Eq. (5.19) starts to play a role ahead of the other terms responsible for transparency of the inner region in which protons are present. Interestingly, this term is a decreasing function of a_n and in some cases acts to cancel an increase of the main term πa_n^2 by an increment of a_n.[14]

6. Empirical Formulas for σ_R

Here, we summarize earlier empirical formulas for σ_R of proton-nucleus reactions, some of which are plotted in Fig. 7 of ref. 2. Since the advent of the geometrical cross section formula designed for collisions of heavy cosmic ray primaries with target nuclei by Bradt and Peters,[15] several formulas have been developed mainly for description of intermediate energy nucleus-nucleus collisions. Kox *et al.* proposed a geometrical formula that expresses σ_R in powers of $A^{1/3}$ by including an energy dependent parameter obtained phenomenologically in the energy range from 30 MeV/nucleon to 2100 MeV/nucleon.[16] The expression for the energy dependent parameter as obtained above was given by Townsend and Wilson.[17] Shen *et al.* extended the formula by Kox *et al*. by taking into account the effect of neutron excess and decreasing the lower limit of its applicable energy range down to a few MeV/nucleon.[18] Tripathi *et al.* further improved the formula by introducing the "medium effect".[19,20] It should be noted that the effect of neutron excess adopted in the last two formulas leads to asymmetry with respect to exchange between projectile and target nuclei.[21]

On the basis of the formula by Bradt and Peters,[15] on the other hand, Sihver *et al.* developed semi-empirical formulas for proton-nucleus (with the target charge $Z_t \leq 26$) and nucleus-nucleus (with the projectile and target charges $Z_p, Z_t \leq 26$) reactions.[22] These formulas are applicable for incident energies above $\simeq$ 15 MeV and $\simeq$ 100 MeV/nucleon, respectively.

There is another genealogy of geometrical formulas for proton-nucleus reaction cross sections. Carlson constructed a formula that is based on a simple geometrical picture by determining the energy-dependent coefficients from empirical data of stable nuclei.[23] The values of these coefficients were parameterized by Machner *et al*.[24] Even earlier than that, a similar empirical formula was constructed for various ion-transport problems of astrophysical interest by Letaw *et al.*[25] Details of these two formulas are given below.

6.1 Carlson's Formula

The expression is given by

$$\sigma_R = \pi\left(R_p + r_0 A^{1/3}\right)^2. \tag{6.1}$$

The values of the coefficients are summarized in Table A of ref. 23. This expression includes an $A^{1/3}$ correction in addition to the simple geometrical $A^{2/3}$ term. Carlson determined this correction in such a way as to reproduce the empirical total reaction cross sections of stable nuclei colliding with protons in the energy range from 40 MeV to 560 MeV.

Machner *et al*. proposed the parametrization of R_p and r_0 as a function of the proton incident energy T_p as in Eqs. (5) and (6) of ref. 24:

$$R_p(T_p) = -0.37 + 5.538\exp(-0.0366T_p), \tag{6.2}$$

and

$$r_0(T_p) = \frac{1}{0.732 + 167.7/T_p^2}, \tag{6.3}$$

with both parameters measured in fm and the energy T_p in MeV. Expression (6.2) overestimates R_p of Eq. (6.1) between $40 \leq T_p \leq 100$ MeV.

6.2 Letaw's Formula

For such high energies as $T_p > 2$ GeV,

$$\begin{aligned}\sigma(T_p) &= \sigma(\mathrm{h.e.})\\ &= 45A^{0.7}[1+0.016\sin(5.3-2.63\ln A)]\ \ \mathrm{mb}.\end{aligned} \tag{6.4}$$

For 2 GeV $> T_p >$ 10 MeV,

$$\begin{aligned}\sigma(T_p) &= \sigma(\mathrm{h.e.})\\ &\quad\times[1-0.62\exp(-T_p/200)\sin(10.9T_p^{-0.28})].\end{aligned} \tag{6.5}$$

where T_p is in units of MeV.

1) A. Kohama, K. Iida, and K. Oyamatsu, Phys. Rev. C **69**, 064316 (2004).
2) A. Kohama, K. Iida, and K. Oyamatsu, J. Phys. Soc. Japan **85** (2016) [The main body of the whole manuscript] [arXiv:1411.7737].
3) A. Kohama, K. Iida, and K. Oyamatsu, Phys. Rev. C **72**, 024602 (2005).
4) H. de Vries, W. de Jager, and C. de Vries, At. Data Nucl. Data Tables **36**, 495 (1987).
5) E. Friedman and A. Gal, Nucl. Phys. **A724**, 143 (2003).
6) G. F. Bertsch and R. A. Broglia, *Oscillations in Finite Quantum Systems* (Cambridge University Press, Cambridge, 1994).
7) A. Bohr and B. R. Mottelson, Nuclear Structure Vol. I *World Scientific*, (1998).
8) H. Kondo, *Master thesis*, Graduate School of Integrated Arts and Sciences, Kochi University (2013) [in Japanese].
9) R. J. Glauber, *Lectures in Theoretical Physics*, Vol. I, ed. W. E. Brittin and D. G. Dunham (Interscience, New York, 1959), p. 315.

10) K. Iida, A. Kohama, and K. Oyamatsu, J. Phys. Soc. Japan **76**, 044201 (2007).
11) L. Spitzer, Jr., *Physical processes in the interstellar medium* (Wiley Classics Library, 1998).
12) G. Royer, Nucl. Phys. **A807**, 105 (2008).
13) L. R. B. Elton and A. Swift, Nucl. Phys. **A94**, 52 (1967).
14) K. Iida, K. Oyamatsu, B. Abu-Ibrahim, and A. Kohama, Prog. Theor. Phys. **126**, 1091 (2011).
15) H. L. Bradt and B. Peters, Phys. Rev. **77**, 54 (1950).
16) S. Kox, A. Gamp, C. Perrin, J. Arvieux, R. Bertholet, J. F. Bruandet, M. Buenerd, R. Cherkaoui, A. J. Cole, Y. El-Masri, N. Longequeue, J. Menet, F. Merchez, and J. B. Viano, Phys. Rev. C **35**, 1678 (1987).
17) L. W. Townsend and J. W. Wilson, Phys. Rev. C **37**, 892 (1988).
18) W. -Q. Shen, B. Wang, J. Feng, W. -L. Zhan, Y. -T. Zhu, and E. -P. Feng, Nucl. Phys. **A491**, 130 (1989).
19) R. K. Tripathi, F. A. Cucinotta, and J. W. Wilson, NASA Technical Paper 3621 (1997).
20) R. K. Tripathi, F. A. Cucinotta, and J. W. Wilson, NASA Technical Paper TP-1999-209726, (1999).
21) L. Sihver, M. Lantz, and A. Kohama, Phys. Rev. C **89**, 067602 (2014).
22) L. Sihver, C. H. Tsao, R. Silberberg, T. Kanai, and A. F. Barghouty, Phys. Rev. C **47**, 1225 (1993).
23) R. F. Carlson, At. Data Nucl. Data Tables **63**, 93 (1996).
24) The GEM collaboration, H. Machner and B. Razen, Nucl. Instru. Meth. **A437**, 419 (1999).
25) J. R. Letaw, R. Silberberg, and C. H. Tsao, Astrophys. J. Suppl., **51**, 271 (1983).